Accepted Manuscript

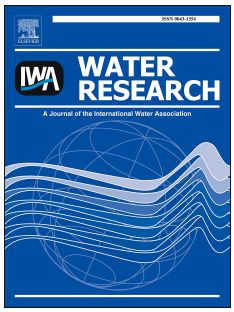

Comparative study on degradation of propranolol and formation of oxidation products by UV/H_2O_2 and UV/persulfate (PDS)

Yi Yang, Ying Cao, Jin Jiang, Xinglin Lu, Jun Ma, Suyan Pang, Juan Li, Yongze Liu, Yang Zhou, Chaoting Guan

PII: S0043-1354(18)30704-8

DOI: https://doi.org/10.1016/j.watres.2018.08.074

Reference: WR 14050

To appear in: *Water Research*

Received Date: 12 April 2018

Revised Date: 22 July 2018

Accepted Date: 31 August 2018

Please cite this article as: Yang, Y., Cao, Y., Jiang, J., Lu, X., Ma, J., Pang, S., Li, J., Liu, Y., Zhou, Y., Guan, C., Comparative study on degradation of propranolol and formation of oxidation products by UV/H_2O_2 and UV/persulfate (PDS), *Water Research* (2018), doi: https://doi.org/10.1016/j.watres.2018.08.074.

Comparative study on degradation of propranolol and formation of oxidation products by UV/H_2O_2 and UV/persulfate (PDS)

Submitted to

Water Research

Yi Yang[1], Ying Cao[1], Jin Jiang[1,*], Xinglin Lu[1,*], Jun Ma[1], Suyan Pang[2], Juan Li[1], Yongze Liu[3], Yang Zhou[1], Chaoting Guan[1]

[1] State Key Laboratory of Urban Water Resource and Environment, Harbin Institute of Technology, Harbin 150090, China

[2] School of Municipal and Environmental Engineering, Jilin Jianzhu University, Changchun 130118, China

[3] School of Environmental Science and Engineering, Beijing Forestry University, Beijing 100083, China

*Corresponding authors:

* E-mail: jiangjinhit@126.com (J. Jiang); xinglin.lu@yale.edu (X. Lu)

ABSTRACT.

The frequent detection of propranolol, a widely used β-blocker, in wastewater effluents and surface waters has raised serious concern, due to its adverse effects on organisms. UV/hydrogen peroxide (UV/H_2O_2) and UV/persulfate (UV/PDS) processes are efficient in eliminating propranolol in various waters, but the formation of oxidation products in these processes, as well as the assessment of their toxicity, has not been systematically addressed. In this study, we identified and compared transformation products of propranolol produced by hydroxyl radical ($^{\bullet}OH$) and sulfate radical ($SO_4^{\bullet-}$). The electrostatic attraction enhances the reaction between $SO_4^{\bullet-}$ and the protonated form of propranolol, while $^{\bullet}OH$ shows non-selectivity toward both protonated and neutral propranolol species. The hydroxylation of propranolol by $^{\bullet}OH$ occurs at either amine moiety or naphthalene group while $SO_4^{\bullet-}$ favors the oxidation of the electron-rich naphthalene group. Further oxidation by $^{\bullet}OH$ and $SO_4^{\bullet-}$ results in ring-opening products. Bicarbonate and chloride exert no effect on propranolol degradation. The generation of $CO_3^{\bullet-}$ and Cl-containing radicals is favorable to oxidizing naphthalene group. The acute toxicity assay of *Vibrio fischeri* suggests that $SO_4^{\bullet-}$ generates more toxic products than $^{\bullet}OH$, while $CO_3^{\bullet-}$ and Cl-containing radicals produce similar toxicity as $SO_4^{\bullet-}$. High concentrations of bicarbonate in UV/H_2O_2 increase the toxicity of treated solution.

Keywords: propranolol; hydroxyl radical; sulfate radical; carbonate radical; Cl-containing radicals; transformation products

Graphical abstract

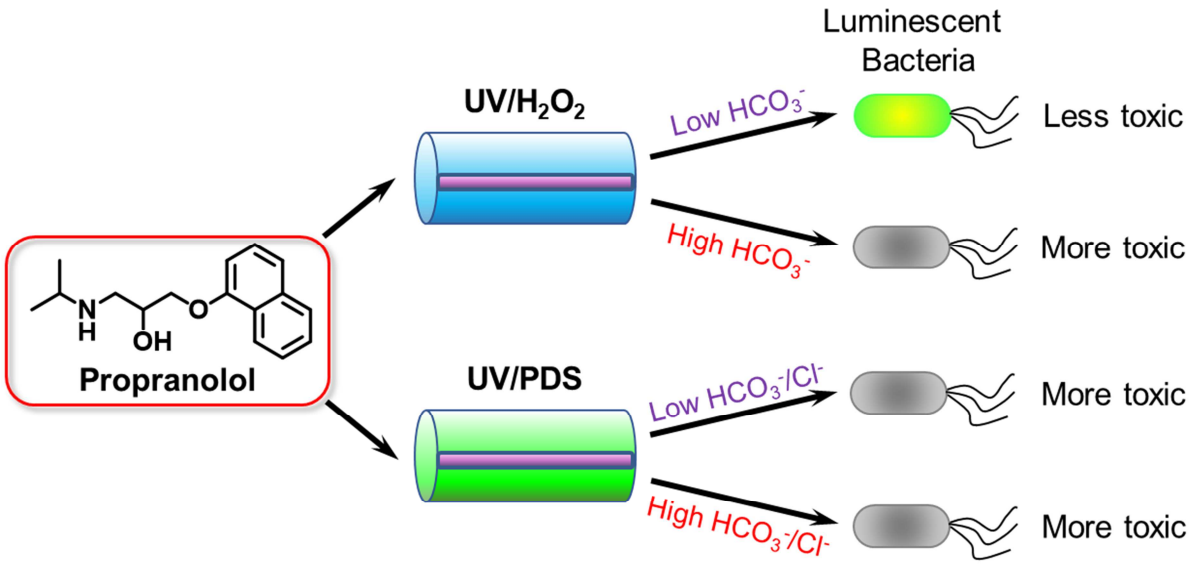

1. Introduction.

As an important class of pharmaceuticals, β-blockers bind to the β-adrenergic receptors in human body and block the action of epinephrine and norepinephrine, which are used to treat cardiac malfunctions.(Khetan and Collins 2007) This target effect of β-blockers to fish with β-adrenergic receptors may exert a similar response to other vertebrates.(Huggett et al. 2002b) β-blockers also exhibit specific nontarget effects on organisms. For example, a previous study demonstrated that three types of β-blocker could inhibit photosynthesis efficiency of a green algae (*Desmodesmus subspicatus*), as echoed by EC_{50} values of 4.1, 40 and 1335 mg/L for propranolol, metoprolol, and atenolol, respectively.(Escher et al. 2006) Another study also indicated the influence of propranolol on the steroid level and reproduction in medaka (*Oryzias latipes*) with exposure to 0.5 μg/L propranolol.(Huggett et al. 2002a) These results suggest that propranolol is more toxic to organisms than other β-blockers. The additive effect of propranolol, which extensively exists in β-blockers mixtures, could contribute to the major toxic potential of overall compounds in the aquatic environment even at low concentrations.(Cleuvers 2005) Additionally, the growing consumption of propranolol in medication and its insufficient removal by conventional WWTPs lead to increasing occurrence of propranolol in surface waters, thereby conceiving substantial concern of its toxicity to aquatic organisms.(Kostich et al. 2014) (Wang et al. 2015)

Advanced oxidation processes (AOPs) are effective in removal of pharmaceuticals.(Keen and Linden 2013, Wols and Hofman-Caris 2012, Zhang et al. 2015) Conventional AOPs typically involve the formation of hydroxyl radicals ($^{\bullet}OH$) as an oxidizing species to destruct recalcitrant organic contaminants in drinking water sources and wastewaters. Recently, sulfate radical-based AOPs have received increasing research interests, as the rate constants for the reaction of sulfate radical ($SO_4^{\bullet-}$) with many organic contaminants are near diffusion-limited rate constants.(Neta et al. 1988) Compared to $^{\bullet}OH$,

the benefit of $SO_4^{\bullet-}$ is its less reactivity to scavengers like bicarbonate and dissolved organic carbon (DOC), which substantially decrease the efficiency of $^{\bullet}OH$-based AOPs through consuming a large portion of $^{\bullet}OH$.(Buxton et al. 1988, Yang et al. 2015) The presence of bicarbonate and halides at high concentrations becomes important scavengers of $^{\bullet}OH$ and $SO_4^{\bullet-}$ to generate daughter reactive species. Unlike $^{\bullet}OH$, $SO_4^{\bullet-}$ favors the conversion of halides to halogen reactive species at neutral pH.(Anipsitakis et al. 2006, Yang et al. 2014) The modeling results showed that inorganic radical concentrations in many wastewaters exceeded those of $^{\bullet}OH$ and $SO_4^{\bullet-}$, especially for $CO_3^{\bullet-}$, by several orders of magnitude.(Grebel et al. 2010, Yang et al. 2014, Zhang et al. 2015) Some halogen reactive species (e.g., $Cl_2^{\bullet-}$) and $CO_3^{\bullet-}$ are more selective oxidants than $^{\bullet}OH$ and $SO_4^{\bullet-}$, but they are capable of oxidizing some organic contaminants.(Beitz et al. 1998, Canonica et al. 2005, Hasegawa and Neta 1978) For instance, our previous results indicated higher reactivity of $CO_3^{\bullet-}$ and halogen reactive species toward propranolol, which led to efficient removal of propranolol by AOPs in various waters.(Yang et al. 2016)

The transformation of propranolol and its product formation by $^{\bullet}OH$-based AOPs (e.g., ozone or photocatalytic by TiO_2) have been well documented, where hydroxylation and ring-opening are the major reaction pathways.(Benner and Ternes 2009, Santiago-Morales et al. 2013, Song et al. 2008) Nevertheless, little study has investigated the transformation of propranolol by $SO_4^{\bullet-}$-based AOPs. The different reactivity between $^{\bullet}OH$ and $SO_4^{\bullet-}$ in the formation and the yield of different products have been demonstrated in the transformation of diclofenac and sulfamethoxazole.(Mahdi Ahmed et al. 2012, Yang et al. 2017, Yu et al. 2013) In these cases, $SO_4^{\bullet-}$ reacts with amine moieties to form corresponding hydroxylamine and nitro moieties, which were not observed in the reaction of $^{\bullet}OH$. Due to the poor mineralization in most applied AOPs, the difference in products formation between these two processes resulted in the discrepancy in toxicity assay.(Yang et al. 2017) Therefore, it is

critical to provide a fundamental understanding of the transformation of propranolol in these AOPs, as well as the toxicity of the formed products, thereby facilitating the application of these AOPs in oxidizing propranolol.

This study aims to compare the transformation of propranolol by $^{\bullet}OH$-based or $SO_4^{\bullet-}$-based AOPs. The rate constants for the reaction of $^{\bullet}OH$ and $SO_4^{\bullet-}$ with propranolol are determined at different pHs. The transformation products are identified to elucidate the reaction pathways. We for the first time systematically compare the effect of bicarbonate and chloride on products formation of propranolol in these two AOPs. The efficiency of propranolol degradation is also evaluated in two authentic water matrices, while reactive species involved in reactions are predicted by kinetic modeling. *Vibrio fisheri* is used in toxicity assay, which is conducted under various operating conditions to evaluate the toxicity of the products in both AOPs.

2. Materials and methods.

2.1. Materials.

Propranolol and ammonium acetate were purchased from Sigma-Aldrich. Sodium perdisulfate (PDS), H_2O_2 solution (35% w/w), *tert*-butanol, sodium chloride and sodium bicarbonate were received from Sinopharm Chemical Reagent Co. Ltd., China. Methanol and acetic acid in HPLC grade were obtained from Thermo Fisher Scientific, and acetonitrile was received from Merck. Stock solutions were prepared in deionized (DI) water (18.2 MΩ/cm) from a Milli-Q purification system (Millipore, Billerica, MA).

2.2. Experimental procedures.

A collimated beam apparatus, consisting of four low-pressure mercury lamp (254 nm, 10 W, GPH212T5L/4, Heraeus) positioned at 30 cm shining down onto a 100 mL crystallization dish (pathlength = 4.0 cm), was used for photolysis experiments, as described previously.(Liu

et al. 2015) The incident photonic flux at 254 nm was 1.291×10^{-7} Einstein L^{-1} s^{-1}, which was determined by the iodide-iodate chemical actinometer.(Rahn et al. 2003) Except when otherwise mentioned, the solution contained PDS or H_2O_2 at 1 mM and propranolol at 20 μM, and was buffered with 10 mM phosphate. Samples (1 mL) were periodically withdrawn and supplemented with 20 μL methanol to quench any radical formed by thermolysis of PDS or H_2O_2, and kept at 4 °C for further analysis within 12 h. Experiments were conducted at 20 ± 2 °C.

The second-order rate constants of propranolol with $^{\bullet}OH$ and $SO_4^{\bullet-}$ were determined by competition kinetics. Atrazine was used as a reference compound for $^{\bullet}OH$ and $SO_4^{\bullet-}$ reactions with $k_{^{\bullet}OH,ATZ} = 2.6 \times 10^9$ M^{-1} s^{-1} and $k_{SO_4^{\bullet-},ATZ} = 2.6 \times 10^9$ M^{-1} s^{-1}, respectively. (Yang et al. 2015) Experiments were conducted according to the aforementioned, except that both propranolol and atrazine were spiked at 5 μM. For the determination of second-order rate constant with $SO_4^{\bullet-}$, 10 mM *tert*-butanol was added to quench $^{\bullet}OH$ in UV/PDS.

Some experiments were conducted using real water samples (i.e., surface water and groundwater) from two drinking water treatment plants. These water samples were filtered through a glass fiber filter (0.7 μm, Whatman) and stored at 4°C. The surface water sample had a low DOC and low alkalinity (DOC 3.8 mg/L, alkalinity 0.2 mM, $[Cl^-]$ = 5.2 mg/L, pH 7.2), while the groundwater sample has relatively higher DOC and alkalinity (DOC 6.9 mg/L, alkalinity 8.0 mM, $[Cl^-]$ = 7.2 mg/L, pH 7.6). Water samples were buffered using 2 mM phosphate. All experiments were conducted in duplicate, and the average values and standard deviations were presented.

2.3. Determination of rate constants for the reactions of propranolol with $^{\bullet}OH$ and $SO_4^{\bullet-}$.

The degradation rate of propranolol by direct photolysis was negligible at pH range of 8–11 in UV/H_2O_2 and UV/PDS (Supplementary data, Fig. S1). To evaluate the specific rate constants for the reactions of $^{\bullet}OH$ and $SO_4^{\bullet-}$ with the protonated and the neutral form of

propranolol, the apparent rate constants ($k_{app,\cdot OH}$ and $k_{app,SO_4^{\cdot-}}$) were determined using competition kinetics at pH ranging from 8 to 11, according to the methods described in Text S1. The initial rate of propranolol and atrazine degradation (degraded fraction of each compound < 20%) was used for calculation to circumvent the competitive effect of their products. The measured $k_{app,\cdot OH}$ and $k_{app,SO_4^{\cdot-}}$ can be expressed as incorporating acid-base speciation of propranolol:

$$k_{app,\cdot OH} = \alpha_{SH_2^+} k_{SH_2^+,\cdot OH} + \alpha_{SH} k_{SH,\cdot OH} \quad (1)$$

$$k_{app,SO_4^{\cdot-}} = \alpha_{SH_2^+} k_{SH_2^+,SO_4^{\cdot-}} + \alpha_{SH} k_{SH,SO_4^{\cdot-}} \quad (2)$$

where $\alpha_{SH_2^+}$ and α_{SH} are the equilibrium distribution coefficients of protonated (SH_2^+) and neutral (SH) forms at a given pH, respectively, and calculated from acidity constant pK_a 9.5.(Benner and Ternes 2009) $k_{SH_2^+,\cdot OH}$, $k_{SH,\cdot OH}$, $k_{SH_2^+,SO_4^{\cdot-}}$ and $k_{SH,SO_4^{\cdot-}}$ are the second-order rate constants for the reactions of $^{\cdot}OH$ and $SO_4^{\cdot-}$ with protonated and neutral forms, respectively. The specific rate constants were calculated through nonlinear regression of experimental data.

2.4. Analytical methods.

Propranolol and atrazine were analyzed by a Waters 1525 HPLC with a Waters 2487 dual λ detector. Chromatographic separations were performed using a Waters Symmetry C18 column (150 mm × 4.6 mm, 5 μm). The concentrations of propranolol and atrazine were quantified at λ = 285 nm and λ = 260 nm, respectively, with an eluent of 0.1% acetic acid and methanol with a ratio of 30:70 (v/v) at a flow rate of 1 mL/min.

Identification of products of propranolol was performed through molecular mass, which was determined by a triple quadrupole TOF mass spectrometer (Triple TOF 5600, AB Sciex) coupled with the Ekspert ultralLC110. A Poroshell 120 EC-C18 column (50 mm × 3.0 mm,

2.7 μm) was used as chromatographic separation. Accurate MS and MS/MS patterns of propranolol and its transformation products were analyzed in both positive and negative electrospray ionization (ESI) modes. The experimental conditions of chromatographic separation and instrumental parameters for HPLC/ Triple TOF are provided in Text S2.

2.5. Kinetic simulations in water samples.

Kinetic modeling of radical concentration for UV/H_2O_2 and UV/PDS processes in two authentic waters was performed using a computer program, Kintecus V6.01.(Ianni 2016) Over one hundred rate constants of elementary reactions were obtained from the literature (Table S3).(Das et al. 1999, Yang et al. 2014, 2016) Due to the lack of sufficient rate constants of many radicals with propranolol, the modeling only took into account the effects of chloride, bicarbonate, and DOC.

2.6. Toxicity analysis.

The acute toxicity assay was carried out by measuring the decrease in the bioluminescence of *Vibrio fischeri*.(Fernández-Alba et al. 2002, Wu et al. 2016, Yang et al. 2017) The measurements were performed using a Promega GloMax®-Multi Jr. The luminescent intensity was determined to calculate the inhibition after 30 min.

3. Results and discussions.

3.1. Oxidation kinetics of the reaction of propranolol with $^{\bullet}OH$ and $SO_4^{\bullet-}$.

The phototransformation quantum yield Φ_{254} of propranolol was determined to be 8.93×10^{-3} at pH 8.3 in our previous study.(Yang et al. 2017) The molar absorption and quantum yield of propranolol were not varied with pH. The photophysical property of propranolol was attributed to the chromophore structure of naphthalene group, which was unlikely affected by pH.(Liu and Williams 2007, Sortino et al. 2002)

The reaction rate constant of propranolol with $^{\bullet}OH$ ($k_{app,^{\bullet}OH}$) was independent of pH

194 from 8 to 11 (Fig. 1A), indicating that $^{\bullet}OH$ exhibited comparable reactivity to both neutral
195 and anionic forms of propranolol. Therefore, the same value of $k_{SH_2^+,^{\bullet}OH}$ and $k_{SH,^{\bullet}OH}$ were
196 suggested here and determined to be $(1.26 \pm 0.10) \times 10^{10}$ M^{-1} s^{-1}, which was consistent with
197 the value of $(1.07 \pm 0.02) \times 10^{10}$ M^{-1} s^{-1} reported in radiolysis experiments.(Song et al. 2008)
198 This value is also comparable to the rate constants determined for the reaction of $^{\bullet}OH$ with
199 naphthalene ($9–12 \times 10^9$ M^{-1} s^{-1}).(Buxton et al. 1988) These results indicated that the reaction
200 of $^{\bullet}OH$ with naphthalene group was predominant, with minimal contribution from the side
201 chain group.

202 Sulfate radical is an electrophile so that a faster rate constant for the reaction of $SO_4^{\bullet-}$
203 with the neutral form of propranolol is expected. However, a continuous decrease in $k_{app,SO_4^{\bullet-}}$
204 with increasing pH from 8 to 11 was observed in Fig. 1B, where $k_{SH_2^+,SO_4^{\bullet-}}$ and $k_{SH,SO_4^{\bullet-}}$ was
205 determined to be $(3.21 \pm 0.08) \times 10^{10}$ M^{-1} s^{-1} and $(1.39 \pm 0.10) \times 10^{10}$ M^{-1} s^{-1}, respectively.
206 Steenken et al. reported that the second-order rate constant for $SO_4^{\bullet-}$ with naphthalene is $2.9 \times$
207 10^9 M^{-1} s^{-1}.(Steenken et al. 1990) The higher rate constant for propranolol may be ascribed to
208 the following two aspects. Due to the electrophilicity of $SO_4^{\bullet-}$, electron-donating substituents
209 like methoxy or hydroxy groups can cause a significant increase in rate constants, which has
210 been demonstrated for substituted benzenes and benzoate ions.(Neta et al. 1977) Therefore,
211 naphthalene substituted by alkoxy group ($(CH_3)_2CNHCH_2CH(OH)CH_2O–$) increases the
212 reactivity of the naphthalene moiety with $SO_4^{\bullet-}$. Additionally, we noticed that these two
213 values approached the diffusion-controlled limit, suggesting that the difference between the
214 expected and the experimental data was likely resulted from the electrostatic attraction
215 between the negatively charged $SO_4^{\bullet-}$ and the positively charged protonation form of
216 propranolol. A previous study also reported that the electrostatic repulsion between $SO_4^{\bullet-}$
217 with the anionic form of organic compounds resulted in lower reaction rate constants than

with the neutral form.(Neta et al. 1977)

3.2. Effect of bicarbonate.

Bicarbonate is an important scavenger of $^{\bullet}OH$ and $SO_4^{\bullet-}$ in the aqueous phase to form carbonate radical ($CO_3^{\bullet-}$) (reactions 3 and 4).(Anastasio and Matthew 2006, Grebel et al. 2010, Yang et al. 2014) Fig. 2 exhibits the effect of bicarbonate on the degradation of propranolol in UV/H_2O_2 and UV/PDS. No difference in propranolol degradation for UV/H_2O_2 was observed as the increase of bicarbonate concentration up to 500 mM. The presence of 5 and 50 mM bicarbonate in UV/PDS showed negligible impact on propranolol degradation kinetics as well, while a marginal decline was observed with the addition of 500 mM bicarbonate. Based on the calculation, 94.5% of $^{\bullet}OH$ and 70% of $SO_4^{\bullet-}$ were scavenged by 500 mM bicarbonate respectively to form $CO_3^{\bullet-}$. Lian et al. reported that the rate constant for the reaction of $CO_3^{\bullet-}$ with propranolol was 1.42×10^7 M^{-1} s^{-1}.(Lian et al. 2017) Although this rate constant is three orders of magnitude lower than those for reaction with $^{\bullet}OH$ and $SO_4^{\bullet-}$, the concentration of $CO_3^{\bullet-}$ appeared to be high enough to fully compensate for the decreased contribution of $^{\bullet}OH$ and $SO_4^{\bullet-}$ to the degradation of propranolol.

$$HCO_3^- + {}^{\bullet}OH \rightarrow CO_3^{\bullet-} + H_2O \qquad k = 8.5 \times 10^6\ M^{-1}\ s^{-1} \qquad (3)$$

$$HCO_3^- + SO_4^{\bullet-} \rightarrow CO_3^{\bullet-} + HSO_4^- \qquad k = 2.8 \times 10^6\ M^{-1}\ s^{-1} \qquad (4)$$

3.3. Effect of chloride.

Chloride is widely present in drinking water and wastewater with various concentrations. The reaction of $^{\bullet}OH$ and $SO_4^{\bullet-}$ with Cl^- generates reactive Cl-containing radicals (e.g., $Cl^{\bullet}$, $Cl_2^{\bullet-}$ and $ClOH^{\bullet-}$). Kinetic modeling in previous studies demonstrated different formation pathways of reactive Cl-containing radicals in UV/H_2O_2 and UV/PDS (Grebel et al. 2010, Yang et al. 2014). The reaction of $^{\bullet}OH$ with Cl^- has a fast rate constant of reverse reaction (reaction 5), where $Cl^{\bullet}$ forms at low pH (reaction 6).(Yang et al. 2014) In contrast, the fast reaction between $SO_4^{\bullet-}$ and Cl^- forms $Cl^{\bullet}$ directly (reaction 7), which can further react with

Cl^- to form other Cl-containing radicals. Since the reaction of $^{\bullet}OH$ with Cl^- was negligible in UV/H_2O_2 at pH 8, (Yang et al. 2016) the effect of Cl^- was only investigated in UV/PDS.

$$Cl^- + {}^{\bullet}OH \rightarrow ClOH^{\bullet-} + H_2O \qquad k_{for} = 4.3 \times 10^9\ M^{-1}\ s^{-1};\ k_{rev} = 6.1 \times 10^9\ M^{-1}\ s^{-1} \qquad (5)$$

$$ClOH^{\bullet-} + H^+ \rightarrow Cl^{\bullet} + H_2O \qquad k_{for} = 2.1 \times 10^{10}\ M^{-1}\ s^{-1} \qquad (6)$$

$$Cl^- + SO_4^{\bullet-} \rightarrow Cl^{\bullet} + SO_4^{2-} \qquad k_{for} = 3.0 \times 10^8\ M^{-1}\ s^{-1} \qquad (7)$$

No significant inhibition of propranolol degradation was observed with Cl^- concentration ranging from 0.1 to 100 mM. In the presence of 100 mM Cl^-, 98% of $SO_4^{\bullet-}$ was scavenged, where Cl-containing radicals were the predominant pathway of propranolol degradation. $Cl^{\bullet}$ and $Cl_2^{\bullet-}$ radicals are strong oxidants ($E(Cl^{\bullet}/Cl^-)$ = 2.4 V and $E(Cl_2^{\bullet-}/2Cl^-)$ = 2.0 V)(Martire et al. 2001) and likely to react with organic compounds.(Hasegawa and Neta 1978) The second-order rate constants for the reaction of $Cl^{\bullet}$ with organic compounds were reported comparably to those of $^{\bullet}OH$ and $SO_4^{\bullet-}$.(NIST) Although $Cl_2^{\bullet-}$ was more selective than $^{\bullet}OH$ and $SO_4^{\bullet-}$ (rate constants of 10^5–$10^9\ M^{-1}\ s^{-1}$),(NIST) the concentration of $Cl_2^{\bullet-}$ could exceed those of $^{\bullet}OH$ and $SO_4^{\bullet-}$ by several orders of magnitude,(Yang et al. 2016) which contributed to the degradation of propranolol.

3.4. Identification of transformation products.

Eleven transformation products (TPs) belonging to nine nominal masses were detected and identified using ESI-TOF-MS. The accurate m/z values are provided in Table 1. The product ion spectra and the fragmentation pathways of propranolol ($[M + H]^+$ = 260.1649) were illustrated in Fig. S2. The m/z 183 fragment ion was resulted from the loss of isopropene, ammonia and water. Fragment ions m/z 155 and m/z 157 corresponded to the cleavage on the side chain and rearrangement of the C–O moiety, which exhibited an unchanged naphthalene group. The m/z 116, 98 and 74 fragment ions were formed by the different cleavages of the side chain. These characteristic fragments of propranolol were important for the comparison with the spectra of TPs as they provide information on the

status of functional groups after oxidation. For structural elucidation, the fragmentation pathways of TPs were investigated by performing product ion scans, which were provided in Fig. S3–S13.

3.4.1. Hydroxyl radical.

Hydroxylation. Due to the negligible degradation of propranolol by direct photolysis, all the nine TPs detected in UV/H_2O_2 were ascribed to the oxidation by $^{\bullet}OH$. The observation of two isomers of TP 275 ($[M + H]^+$ = 276.1594) was owing to the addition of one oxygen atom to propranolol molecule. The product ion scan of TP 275-1 showing two sequential loss of water (fragment ions m/z 258 and 240) could signify two hydroxyl moieties, which were present next to a removable proton. This result implied that amine moiety was likely hydroxylated to form a hydroxylamine product. The fragment ion m/z 173 of TP 275-2 was formed through hydroxylation on naphthalene group of m/z 157, thereby indicating the oxidation of the naphthalene group on propranolol. The occurrence of m/z 116 and 98 fragment ions provided further support on the proposed fragment pathway. The difference in molecular weight of propranolol and TP 291-1 ($[M + H]^+$ = 292.1543) was 32 Da, corresponding to the addition of two oxygen atoms. The loss of 60 Da (i.e., 18 + 42 Da) suggested the cleavage of water and isopropyl moiety. Double hydroxylation on the ring was supported by the fragment ion m/z 175, corresponding to the cleavage of C–O moiety and two hydroxylated groups on the ring.

Ring-opening. Several peaks with a nominal mass of 307 Da were observed. TP 307 ($[M + H]^+$ = 308.1492) was resulted from the addition of three oxygen atoms (+48 Da) to propranolol. The product ion scan showing two sequential loss of water (fragment ions m/z 290 and 272) signified that two hydroxyl moieties were present next to a removable proton, implying one hydroxylation on the side chain. Hydroxylation next to either ethoxy group or amine moiety would cause an unstable hemiaminal.(Benner and Ternes 2009) Hence, the

amine moiety was likely hydroxylated, thus leading to the formation of hydroxylamine. The m/z 175 fragment ion corresponded to the addition of two oxygen atoms on the naphthalene group. The proposed formation of two aldehyde moieties rather than a double hydroxylation was supported by the fragment ion m/z 131 (175-131=44 Da, loss of CO_2). The structure of TP 281 ($[M + H]^+$ = 282.1336) was also a ring-opening product with the occurrence of m/z 149, indicating the formation of two aldehyde moieties. Only one loss of water (fragment ion m/z 264) confirmed the hydroxylation of the naphthalene group. TP 293 ($[M + H]^+$ = 294.1700) showed one less double bond than TP 291-1. The unchanged side chain can be seen by the single loss of water (fragment ion m/z 276). The fragment ions m/z 199 and m/z 173 had quinone-like structure, which derived from dehydration of one aldehyde moiety and one hydroxyl group in the aromatic structure. TP 309 ($[M + H]^+$ = 310.1649) showed two isomers. The fragment ion m/z 177 was resulted from the cleavage of the C-O bond, indicating that the addition of three oxygen atoms took place at the aromatic structure and no oxidation on the side chain. The second loss of water (fragment ion m/z 274) suggested that the hydroxyl group on the aromatic structure was present next to a removable proton. The second hydroxyl group can either occur in a carboxyl moiety or at other positions of the ring. However, no carboxyl moiety was detected in negative ionization mode. The detection of TP 309 in the positive mode was likely ascribed to a hydroxylation of the ring. The appearance of fragment ion m/z 114 demonstrated the ring-opening of the naphthalene group at 3,4-position.

Cleavage. The fragment ions m/z 116 and 74 of TP 133 ($[M + H]^+$ = 134.1176) were formed by the loss of water and isopropyl group, indicating two hydroxyl groups of the structure. The structure of TP 166 ($[M - H]^-$ = 165.0193) was proposed to form two carboxyl moieties, which was supported by the fragment ion m/z 121 (165-121=44 Da, loss of CO_2) and 77 (121-77=44 Da, loss of CO_2).

3.4.2. Sulfate radical.

Seven TPs detected in UV/PDS were ascribed to the oxidation by $SO_4^{\bullet-}$, where TP 133, TP 166, TP 275-2, TP 307 and TP 309 were similar to those in UV/H_2O_2. TP 273 ($[M + H]^+$ = 274.1437) corresponded to the addition of one oxygen atom to propranolol molecule with one more double bond than TP 275. The fragment ion m/z 159 indicated the oxidation of naphthalene group. A fragment ion m/z 131 was ascribed to a loss of CO of m/z 159. Hence, the occurrence of double bond most likely took place on the side chain. An isomer of TP 291-1 with different retention time and MS/MS spectra was denoted as TP 291-2. The difference could be explained by the formation of two aldehyde moieties rather than double hydroxylation on the ring, which was supported by the occurrence of m/z 131 and 103 through two sequential loss of CO (159-131=28 Da, and 131-103=28 Da).

3.4.3. Carbonate radical and chlorine radicals.

The addition of 50 and 500 mM bicarbonate in UV/H_2O_2 inhibited the formation of TP 291-1. Neither TP 275-1 nor TP 293 was observed in the presence of 500 mM bicarbonate, while TP 273 was generated. In such a condition, $CO_3^{\bullet-}$ was the dominant radical. Thus the formation of TPs was attributed to the oxidation of propranolol by $CO_3^{\bullet-}$.

For UV/PDS, neither bicarbonate nor low concentration of Cl^- affected the formation of TPs. TP 275-1 appeared at high concentration of Cl^-, which was due to the conversion of $Cl^\bullet$ to $^\bullet$OH (see discussion below). TPs generated by $CO_3^{\bullet-}$ and Cl-containing radicals were similar to those by $SO_4^{\bullet-}$, indicating that the reaction pathways of propranolol degradation by $SO_4^{\bullet-}$ occurred for $CO_3^{\bullet-}$ and Cl-containing radicals.

3.5. Proposed transformation pathway.

$^\bullet$OH pathway. $^\bullet$OH attacks the naphthalene group of propranolol to form a carbon-centered radical, which further reacts with oxygen to generate a peroxy radical and subsequent forms a hydroxylated product (TP 291-1, Scheme 1). The oxidation of this

product is followed by ring-opening and the formation of aldehyde moieties to produce TP 291-2. $^{\bullet}$OH attacks the aldehyde moiety, leading to the formation of alcohol or/and carboxyl group, namely TP 293 and TP 309. Additionally, the double bond is likely attacked by $^{\bullet}$OH in the α-position of the aldehyde moiety by cleavage of acetaldehyde to form TP 281. Even though several isomers of TP 281 were proposed, only one signal was detected. The cleavage of ether bond on propranolol and its products generates TP 133 and TP166.

$SO_4^{\bullet-}$ pathway. The pK_a of propranolol is 9.5, implying lower reactivity of protonated amine group at pH 8. Due to the electrophilic property of $SO_4^{\bullet-}$, it favors the oxidation of the naphthalene group rather than the amine group, which leads to the formation of TP 275-2 rather than TP 275-1 (Scheme 1). The amine moiety could be considered as a secondary reactive site when the oxidized naphthalene group is less reactive (i.e., TP 307). Hydroxyl as an electron-donating group on naphthalene facilitates further oxidation on its ortho-position by $SO_4^{\bullet-}$, resulting in a ring-opening product (TP 291-2). Alternatively, the less selectivity of $^{\bullet}$OH leads to the formation of multi-hydroxyl products (TP 291-1), which may occur on different benzene rings. The formation of TP 273 is not clear, which may involve dehydration of the side chain.

$CO_3^{\bullet-}$ and Cl-containing radicals pathway. $CO_3^{\bullet-}$ and $Cl_2^{\bullet-}$ are more selective oxidants compared with $^{\bullet}$OH and $SO_4^{\bullet-}$,(Buxton et al. 1988, Neta et al. 1988, Neta et al. 1977) thus reacting with organic compounds mainly through electron transfer, which is similar to that of $SO_4^{\bullet-}$. Despite the fact that $Cl^{\bullet}$ exhibits high reactivity toward organic compounds, which is similar to $^{\bullet}$OH, $Cl^{\bullet}$ could not be considered as a dominant radical in the system. Not only the faster reverse rate of reaction 5 favors the formation of $^{\bullet}$OH at neutral pH, but also the excess Cl^- consumes $Cl^{\bullet}$ to form $Cl_2^{\bullet-}$.

When $CO_3^{\bullet-}$ is the dominant radical in both UV/H_2O_2 and UV/PDS, the same products are formed as those by $SO_4^{\bullet-}$. With a low concentration of Cl^- (0.1 mM), most $SO_4^{\bullet-}$ reacts

with propranolol, while only 4.5% of $SO_4^{\bullet-}$ reacts with Cl^- to generate $Cl^\bullet$. Therefore, no effect was noticed on product formation compared with $SO_4^{\bullet-}$. As Cl^- concentration increased, the formation of TP 275-1 was observed, which is likely ascribed to the oxidation by either $^\bullet OH$ or $Cl^\bullet$. Previous studies demonstrated that as Cl^- concentration varied from 33 to 540 mM, the steady-date concentration of $^\bullet OH$ was three to five orders of magnitude higher than that of $Cl^\bullet$.(Yang et al. 2014, 2016) Since the rate constant of $^\bullet OH$ with propranolol is near the diffusion-controlled limit, $^\bullet OH$ is believed to the dominant oxidant contributing to the degradation of propranolol rather than $Cl^\bullet$, leading to the formation of TP 275-1.

3.6. Oxidation in authentic water matrices.

The degradation of propranolol in groundwater was slightly slower than that in surface water for both UV/H_2O_2 and UV/PDS. This opposite effect of bicarbonate in authentic vs. simulated waters was likely ascribed to the scavenging effect of reactive components in authentic waters (*e.g.*, DOC). Kinetic modeling of steady-state concentration of radicals in two authentic water matrices was shown in Table 2. A higher DOC concentration in groundwater decreased the concentration of radicals except for $CO_3^{\bullet-}$. Although the concentration of $CO_3^{\bullet-}$ was one or two orders of magnitude higher than that of $^\bullet OH$ or $SO_4^{\bullet-}$ in groundwater, the rate constant of $CO_3^{\bullet-}$ with propranolol was three orders of magnitude lower than that of $^\bullet OH$ or $SO_4^{\bullet-}$. Therefore, $^\bullet OH$ or $SO_4^{\bullet-}$ was the dominant radical in both groundwater and surface water, and their relatively low concentration in groundwater reduced the propranolol degradation rate. As the yield of $SO_4^{\bullet-}$ (1.4) in UV/PDS was higher than that of $^\bullet OH$ (1.0) in UV/H_2O_2,(Baxendale and Wilson 1957, Mark et al. 1990) the degradation of propranolol was faster in UV/PDS than that in UV/H_2O_2 in both water matrices.

Similar products were found in two water matrices (Fig. 4). TP 281 and TP 291-1 were only observed in UV/H_2O_2, while TP 275-1 was not detected in any condition. A higher concentration of CO_3^{2-} inhibited the formation of TP 291-1, confirming that hydroxylation

was the dominant pathway of $^{\bullet}OH$. The maximum concentrations of TP 273 and TP 275-2 in UV/PDS were higher than those in UV/H_2O_2, consisting with the results in the simulated waters. The sharp decrease of these two products was observed by UV/PDS in surface water, although the degradation rate of propranolol in two water matrices was similar. This result indicates that $SO_4^{\bullet-}$ was a stronger oxidant than $CO_3^{\bullet-}$ to further oxidize these products. Similar trends of products formation were also noticed for TP 291-2, TP 293, TP 307 and TP 309. The maximum concentrations of TP 293, TP 307 and TP 309 in UV/H_2O_2 were higher than those in UV/PDS, while the faster degradations of products were found in surface water rather than those in groundwater, owing to the further oxidation of products by $^{\bullet}OH$. The higher concentration of the cleavage product TP 133 by UV/H_2O_2 was due to the different reactivity of $^{\bullet}OH$ and $SO_4^{\bullet-}$ toward the side chain. In groundwater, both TP 166 and TP 291-2 exhibited higher concentration than those in surface water, which was likely attributed to either the lower reactivity of $CO_3^{\bullet-}$ toward these products, or the oxidation of their precursors by $^{\bullet}OH$ and $SO_4^{\bullet-}$. These comparisons between two matrices simulated the formation of products in real-world applications of these two AOPs.

3.7. Acute toxicity of transformation products in UV-based AOPs.

Microtox assay has been widely employed to determine the acute toxicity of substances in the environment. A model marine bacterium of *Vibrio fischeri* was selected herein as an indicator of toxicity, because it is tolerant to the high concentration of salts used in this study (100 mM bicarbonate or Cl^-). The acute toxicity was expressed by the luminescence inhibition of *Vibrio fischeri* in the treatment of propranolol via different procedures (Fig. 5). L_0 was the luminescence of propranolol without treatment, while L was the luminescence of samples with corresponding treatments and conditions. The acute toxicity was determined by the ratio of L/L_0, where a lower value implies higher acute toxicity, and *vice versa*. The dashed line represented the luminescence of residual propranolol in a sample.

With the decrease of propranolol in UV/H_2O_2, the inhibition effects on *Vibrio fischeri* decreased up to 20% relative to the initial luminescence. This result was consistent with the toxicity of residual propranolol, which can be explained by the fewer toxic products generated by $^{\bullet}OH$. In UV/PDS, 20% degradation of propranolol led to ~80% inhibition of luminescence. When propranolol was removed by 40%, the luminescence was completely inhibited, suggesting that the products generated by $SO_4^{\bullet-}$ were more toxic than propranolol.

The effects of oxidation products of $CO_3^{\bullet-}$ or Cl-containing radicals were also shown in Fig. 5. The concentration of bicarbonate or Cl^- at 100 mM was used to create a background with dominant $CO_3^{\bullet-}$ or Cl-containing radicals. The presence of bicarbonate in UV/ H_2O_2 showed no luminescence inhibition when the removal of propranolol was less than 30%. However, the toxicity sharply increased as the degradation of propranolol proceeded. Bicarbonate at 100 mM could scavenge 77% of $^{\bullet}OH$, implying that $^{\bullet}OH$ contributed to the partial degradation of propranolol and the formation of its corresponding products. The non-effect on *Vibrio fischeri* in the initial phase could be explained by two possible reasons: either $^{\bullet}OH$ generated fewer toxic products, or the accumulation of toxic products by $CO_3^{\bullet-}$ was not sufficient to affect the overall toxicity. Subsequently, the further oxidation of products by $^{\bullet}OH$ or $CO_3^{\bullet-}$ generated more toxic products. The presence of bicarbonate or Cl-containing radicals in UV/PDS exhibited comparable toxicity to that in UV/PDS. Taken together, these results indicated that the products generated by $SO_4^{\bullet-}$, $CO_3^{\bullet-}$ or Cl-containing radicals were more toxic than those by $^{\bullet}OH$.

4. Conclusions.

Hydroxyl radical showed unselective oxidation towards propranolol species. Although $SO_4^{\bullet-}$ was expected to be more reactive toward the neutral form of propranolol, the electrostatic attraction between $SO_4^{\bullet-}$ and the protonated form of propranolol could facilitate

this reaction. $^{\bullet}OH$ reacted with either amine moiety or naphthalene group through hydroxylation pathway, which underwent further oxidation to form ring-opening products. $SO_4^{\bullet-}$ exhibited high reactivity toward the electron-rich naphthalene group. When the oxidized naphthalene group was less reactive, the amine moiety as a secondary reactive site could be oxidized by $SO_4^{\bullet-}$. The same products through the cleavage of the side chain were observed in both AOPs. Neither bicarbonate nor Cl^- had a significant effect on propranolol degradation. $CO_3^{\bullet-}$ and Cl-containing radicals were favorable in oxidizing the naphthalene group. Since $Cl_2^{\bullet-}$ played a role in the conversion of $SO_4^{\bullet-}$ to $^{\bullet}OH$, the characteristic product by $^{\bullet}OH$ was detected at high concentrations of Cl^- in UV/PDS. The acute toxicity assay implied that the products generated by $SO_4^{\bullet-}$ were more toxic than those by $^{\bullet}OH$. $CO_3^{\bullet-}$ and Cl-containing radicals gave similar toxic products as $SO_4^{\bullet-}$. The presence of bicarbonate in UV/H_2O_2 enhanced the generation of toxic products. It should be noted that the toxicity of specific product needs to be further identified, which will facilitate a better understanding of toxicological potential when these AOPs are applied in treating waters with different backgrounds.

Appendix A. Supplementary data

Supplementary data related to this article can be found at:

Acknowledgments

We acknowledge the Chinese International Postdoctoral Exchange Fellowship Program (No. 20160074) for support for Y.Y. We are thankful for the Excellent Graduate Student Scholarship from the Shanghai Tongji Gao Tingyao Environmental Science and Technology Development Foundation awarded to X. Lu.

467 **Figures and tables.**

468

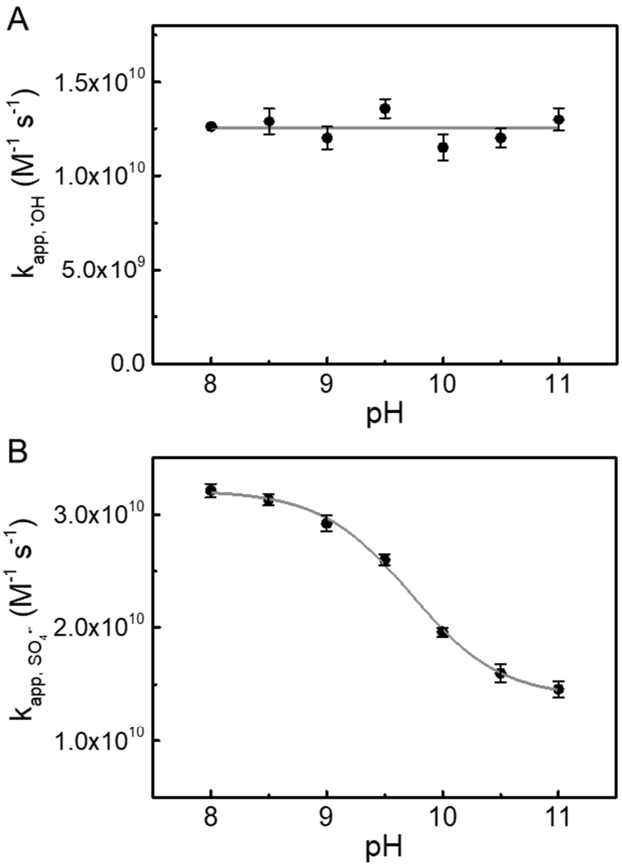

469

470 **Fig. 1.** Apparent second-order rate constants for the reactions of propranolol with (A) $^{\bullet}OH$

471 and (B) $SO_4^{\bullet-}$.

472

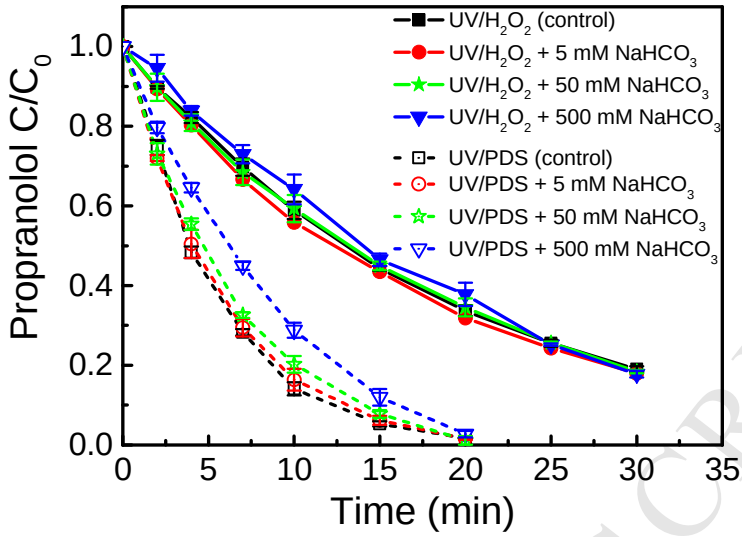

Fig. 2. Effect of bicarbonate on degradation of propranolol in UV/H_2O_2 or UV/PDS at pH 8. Experimental condition: $[propranolol]_0$ = 20 μM, and $[H_2O_2]_0$ or $[PDS]_0$ =1 mM.

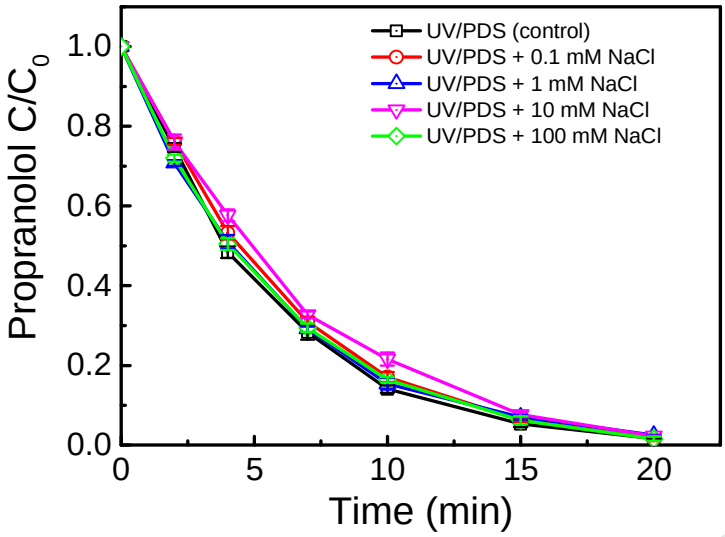

478

479 **Fig. 3.** Effect of chloride on degradation of propranolol in UV/PDS at pH 8. Experimental

480 condition: $[propranolol]_0$ = 20 μM, and $[PDS]_0$ =1 mM.

481

482 **Table 1.** Products detected by TOF-MS in UV/H_2O_2 and UV/PDS.

Product ID	RT (min)	ESI (+/-)	Observed Mass	Calculated Mass	Molecular formula	Proposed structure
Propranolol	13.8	+	260.16491	260.16451	C16H21NO2	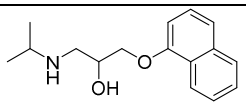
TP 133	1.1	+	134.11756	134.11761	C14H19NO5	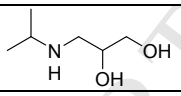
TP 166	0.9	-	165.01933	165.01934	C8H6O4	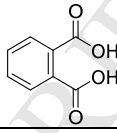
TP 273	11.0	+	274.14377	274.144	C16H19NO3	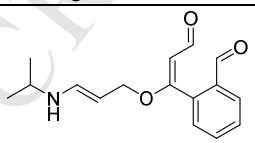
TP 275-1	2.5	+	276.15942	276.16687	C16H21NO3	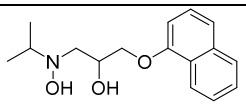
TP 275-2	9.6	+	276.15942	276.16687	C16H21NO3	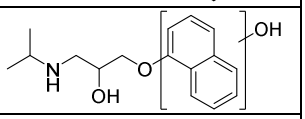
TP 281	1.1	+	282.1336	282.13387	C14H19NO5	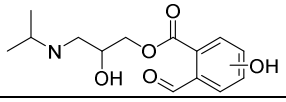
TP 291-1	1.7	+	292.15433	292.15295	C16H21NO4	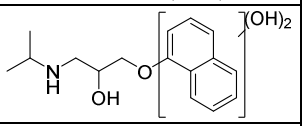
TP 291-2	10.3	+	292.15433	292.15295	C16H21NO4	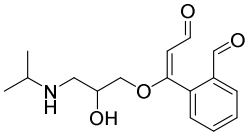
TP 293	2.5	+	294.16998	294.17032	C16H23NO4	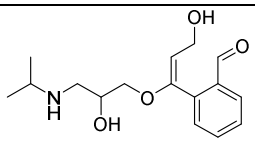
TP 307	1.7 3.1 4.0	+	308.14925	308.14981	C16H21NO5	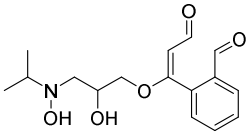
TP 309	1.6 2.9	+	310.1649	310.16515	C16H23NO5	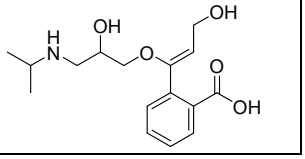

483

484

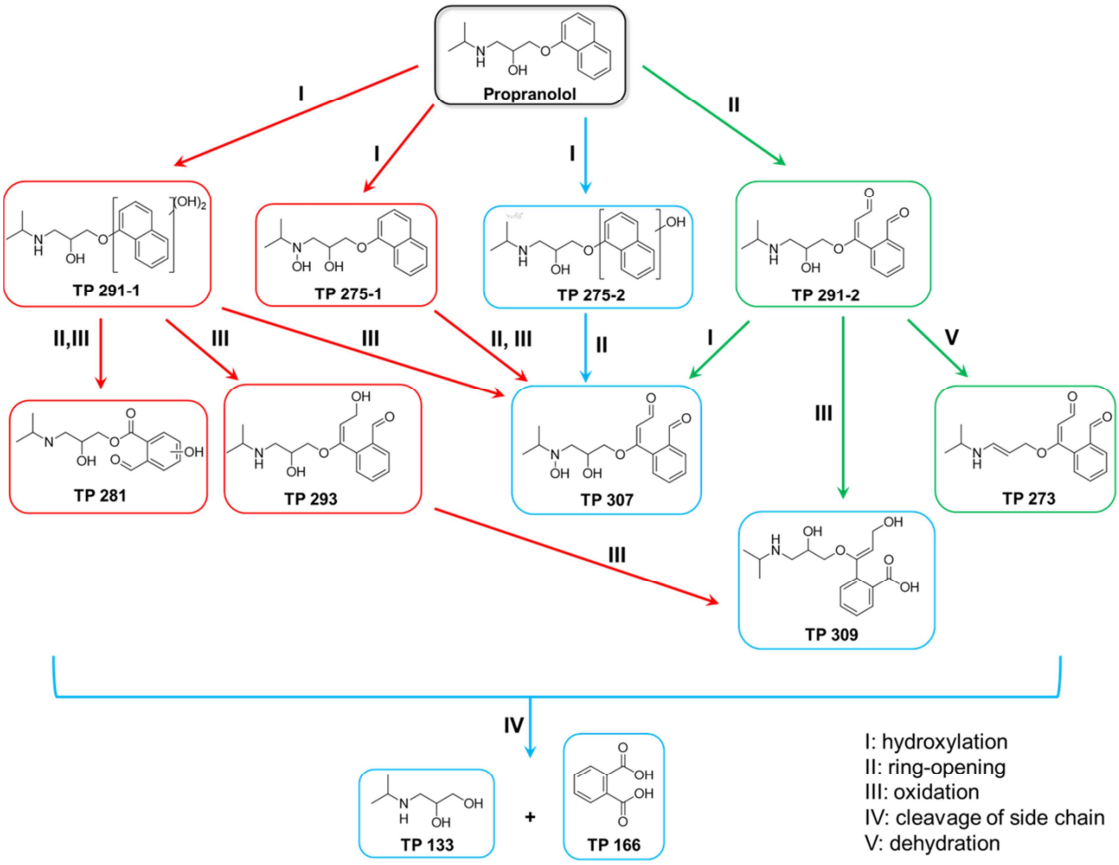

485

486 **Scheme 1.** Proposed degradation pathways for propranolol by $^{\bullet}OH$, $SO_4^{\bullet-}$, $CO_3^{\bullet-}$ and Cl-
487 containing radicals. Red boxes indicated the generation of products by $^{\bullet}OH$; green boxes
488 indicated the generation of products by $SO_4^{\bullet-}$, $CO_3^{\bullet-}$ and Cl-containing radicals; blue boxes
489 indicated the generation of products in all processes.

490

491

492 **Table 2.** Modeled molar concentrations of inorganic radicals for various water matrices [a]

Reactive species (M)	UV/H_2O_2		UV/PDS	
	Groundwater	Surface water	Groundwater	Surface water
$[SO_4^{\bullet-}]$			2.20E-13	4.03E-13
$[^{\bullet}OH]$	6.67E-14	1.35E-13	4.19E-14	1.57E-13
$[Cl^{\bullet}]$	2.62E-22	4.42E-22	7.80E-16	1.21E-15
$[Cl_2^{\bullet-}]$	6.31E-22	3.86E-21	1.80E-15	1.03E-14
$[CO_3^{\bullet-}]$	1.95E-12	1.50E-13	4.51E-12	4.72E-13

493 a. Simulation without propranolol. Simulation time = 5 min, 1 mM H_2O_2 or 1 mM PDS.

494

495

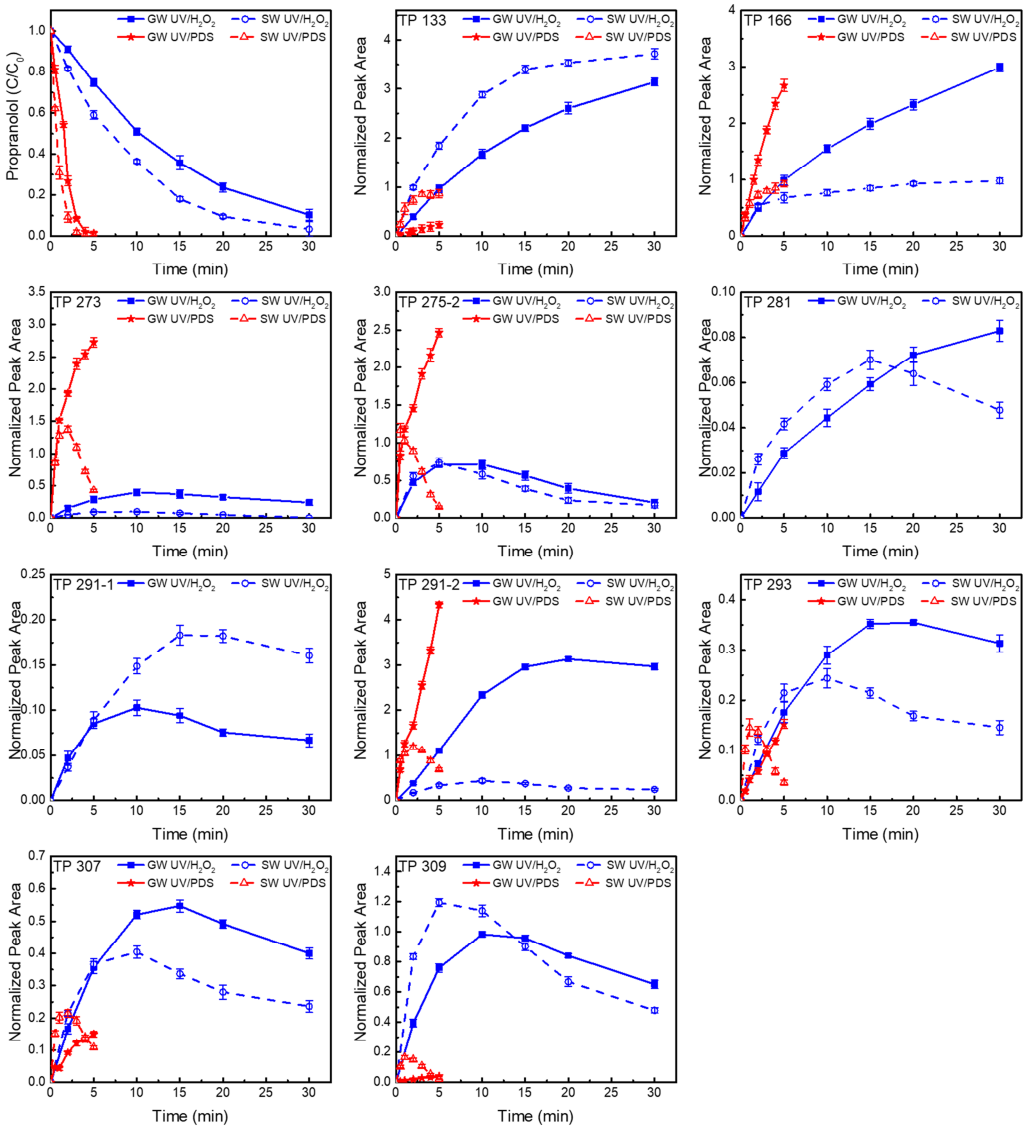

Fig. 4. Propranolol degradation and main transformation products (TPs) formation in authentic waters. GW and SW represent the groundwater and the surface water, respectively. Peak areas were normalized to the peak area of the internal standard. Experimental condition: $[propranolol]_0$ = 1 μM, $[H_2O_2]_0$ or $[PDS]_0$ = 1 mM.

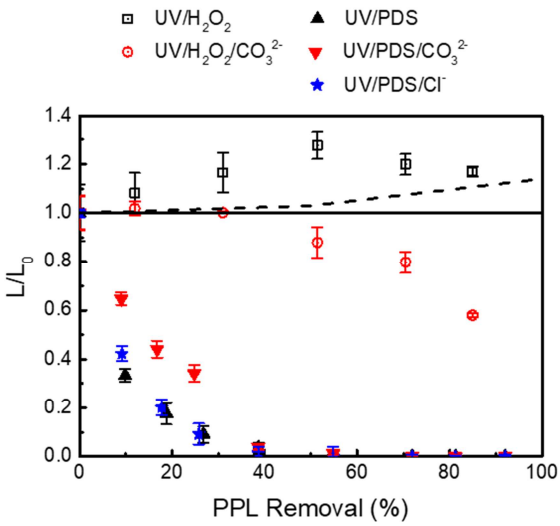

503

504 **Fig. 5.** Impact on *Vibrio fischeri* luminescence by propranolol after different treatments
505 with/without bicarbonate or chloride. The dash line represents the luminescence induced by
506 the remaining propranolol. Errors represent the standard deviation (n = 4). Experimental
507 condition: $[propranolol]_0$ = 20 μM, $[HCO_3^-]$ or $[Cl^-]$ = 100 mM, $[H_2O_2]_0$ or $[PDS]_0$ =1 mM.

508

509

References

Anastasio, C. and Matthew, B.M. (2006) A chemical probe technique for the determination of reactive halogen species in aqueous solution: Part 2 - chloride solutions and mixed bromide/chloride solutions. Atmospheric Chemistry and Physics 6, 2439-2451.

Anipsitakis, G.P., Dionysiou, D.D. and Gonzalez, M.A. (2006) Cobalt-Mediated Activation of Peroxymonosulfate and Sulfate Radical Attack on Phenolic Compounds. Implications of Chloride Ions. Environmental Science & Technology 40(3), 1000-1007.

Baxendale, J. and Wilson, J. (1957) The photolysis of hydrogen peroxide at high light intensities. Transactions of the Faraday Society 53, 344-356.

Beitz, T., Bechmann, W. and Mitzner, R. (1998) Investigations of Reactions of Selected Azaarenes with Radicals in Water. 2. Chlorine and Bromine Radicals. The Journal of Physical Chemistry A 102(34), 6766-6771.

Benner, J. and Ternes, T.A. (2009) Ozonation of Propranolol: Formation of Oxidation Products. Environmental Science & Technology 43(13), 5086-5093.

Buxton, G.V., Greenstock, C.L., Helman, W.P. and Ross, A.B. (1988) Critical review of rate constants for reactions of hydrated electrons, hydrogen atoms and hydroxyl radicals. Journal of Physical and Chemical Reference Data 17(2), 513-886.

Canonica, S., Kohn, T., Mac, M., Real, F.J., Wirz, J. and von Gunten, U. (2005) Photosensitizer method to determine rate constants for the reaction of carbonate radical with organic compounds. Environmental Science & Technology 39(23), 9182-9188.

Cleuvers, M. (2005) Initial risk assessment for three β-blockers found in the aquatic environment. Chemosphere 59(2), 199-205.

Das, T.N., Huie, R.E. and Neta, P. (1999) Reduction Potentials of SO3•-, SO5•-, and S4O6•3- Radicals in Aqueous Solution. The Journal of Physical Chemistry A 103(18), 3581-3588.

Escher, B.I., Bramaz, N., Richter, M. and Lienert, J. (2006) Comparative Ecotoxicological Hazard Assessment of Beta-Blockers and Their Human Metabolites Using a Mode-of-Action-Based Test Battery and a QSAR Approach. Environmental Science & Technology 40(23), 7402-7408.

Fernández-Alba, A.R., Hernando, D., Agüera, A., Cáceres, J. and Malato, S. (2002) Toxicity assays: a way for evaluating AOPs efficiency. Water Research 36(17), 4255-4262.

Grebel, J.E., Pignatello, J.J. and Mitch, W.A. (2010) Effect of halide ions and carbonates on organic contaminant degradation by hydroxyl radical-based advanced oxidation processes in saline waters. Environmental Science & Technology 44(17), 6822-6828.

Hasegawa, K. and Neta, P. (1978) Rate Constants and Mechanisms of Reaction of Cl2- Radicals. Journal of Physical Chemistry 82(8), 854-857.

Huggett, D., Brooks, B., Peterson, B., Foran, C. and Schlenk, D. (2002a) Toxicity of select beta adrenergic receptor-blocking pharmaceuticals (B-blockers) on aquatic organisms. Archives of Environmental Contamination and Toxicology 43(2), 229-235.

Huggett, D.B., Brooks, B.W., Peterson, B., Foran, C.M. and Schlenk, D. (2002b) Toxicity of Select Beta Adrenergic Receptor-Blocking Pharmaceuticals (B-Blockers) on Aquatic Organisms. Archives of Environmental Contamination and Toxicology 43(2), 229-235.

Ianni, J.C. (2016) Kintecus V6.01. www.kintecus.com.

Keen, O.S. and Linden, K.G. (2013) Degradation of Antibiotic Activity during UV/H2O2 Advanced Oxidation and Photolysis in Wastewater Effluent. Environmental Science & Technology 47(22), 13020-13030.

Khetan, S.K. and Collins, T.J. (2007) Human pharmaceuticals in the aquatic

environment: a challenge to green chemistry. Chemical Reviews 107(6), 2319-2364.

Kostich, M.S., Batt, A.L. and Lazorchak, J.M. (2014) Concentrations of prioritized pharmaceuticals in effluents from 50 large wastewater treatment plants in the US and implications for risk estimation. Environmental Pollution 184, 354-359.

Lian, L., Yao, B., Hou, S., Fang, J., Yan, S. and Song, W. (2017) Kinetic Study of Hydroxyl and Sulfate Radical-Mediated Oxidation of Pharmaceuticals in Wastewater Effluents. Environmental Science & Technology 51(5), 2954-2962.

Liu, Q.-T. and Williams, H.E. (2007) Kinetics and Degradation Products for Direct Photolysis of β-Blockers in Water. Environmental Science & Technology 41(3), 803-810.

Liu, Y., Jiang, J., Ma, J., Yang, Y., Luo, C., Huangfu, X. and Guo, Z. (2015) Role of the propagation reactions on the hydroxyl radical formation in ozonation and peroxone (ozone/hydrogen peroxide) processes. Water Research 68, 750-758.

Mahdi Ahmed, M., Barbati, S., Doumenq, P. and Chiron, S. (2012) Sulfate radical anion oxidation of diclofenac and sulfamethoxazole for water decontamination. Chemical Engineering Journal 197, 440-447.

Mark, G., Schuchmann, M.N., Schuchmann, H.-P. and von Sonntag, C. (1990) The photolysis of potassium peroxodisulphate in aqueous solution in the presence of tert-butanol: a simple actinometer for 254 nm radiation. Journal of Photochemistry and Photobiology A: Chemistry 55(2), 157-168.

Martire, D.O., Rosso, J.A., Bertolotti, S., Le Roux, G.C., Braun, A.M. and Gonzalez, M.C. (2001) Kinetic study of the reactions of chlorine atoms and Cl(2)(center dot-)radical anions in aqueous solutions. II. Toluene, benzoic acid, and chlorobenzene. Journal of Physical Chemistry A 105(22), 5385-5392.

Neta, P., Huie, R.E. and Ross, A.B. (1988) Rate constants for reactions of inorganic radicals in aqueous solution. Journal of Physical and Chemical Reference Data 17(3), 1027-1284.

Neta, P., Madhavan, V., Zemel, H. and Fessenden, R.W. (1977) Rate constants and mechanism of reaction of sulfate radical anion with aromatic compounds. Journal of the American Chemical Society 99(1), 163-164.

NIST (2017) NDRL/NIST Solution Kinetics Database on the Web. http://kinetics.nist.gov/solution/ (Accessed September, 2017).

Rahn, R.O., Stefan, M.I., Bolton, J.R., Goren, E., Shaw, P.S. and Lykke, K.R. (2003) Quantum yield of the iodide-iodate chemical actinometer: Dependence on wavelength and concentration. Photochemistry and Photobiology 78(2), 146-152.

Santiago-Morales, J., Agüera, A., Gómez, M.d.M., Fernández-Alba, A.R., Giménez, J., Esplugas, S. and Rosal, R. (2013) Transformation products and reaction kinetics in simulated solar light photocatalytic degradation of propranolol using Ce-doped TiO2. Applied Catalysis B: Environmental 129, 13-29.

Song, W., Cooper, W.J., Mezyk, S.P., Greaves, J. and Peake, B.M. (2008) Free Radical Destruction of β-Blockers in Aqueous Solution. Environmental Science & Technology 42(4), 1256-1261.

Sortino, S., Petralia, S., Bosca, F. and Miranda, M.A. (2002) Irreversible photo-oxidation of propranolol triggered by self-photogenerated singlet molecular oxygen. Photochemical & Photobiological Sciences 1(2), 136-140.

Steenken, S., Warren, C.J. and Gilbert, B.C. (1990) Generation of radical-cations from naphthalene and some derivatives, both by photoionization and reaction with SO 4–˙: formation and reactions studied by laser flash photolysis. Journal of the Chemical Society, Perkin Transactions 2 (2), 335-342.

Wang, B., Dai, G., Deng, S., Huang, J., Wang, Y. and Yu, G. (2015) Linking the

environmental loads to the fate of PPCPs in Beijing: Considering both the treated and untreated wastewater sources. Environmental Pollution 202, 153-159.

Wols, B.A. and Hofman-Caris, C.H.M. (2012) Review of photochemical reaction constants of organic micropollutants required for UV advanced oxidation processes in water. Water Research 46(9), 2815-2827.

Wu, Z., Fang, J., Xiang, Y., Shang, C., Li, X., Meng, F. and Yang, X. (2016) Roles of reactive chlorine species in trimethoprim degradation in the UV/chlorine process: Kinetics and transformation pathways. Water Research 104, 272-282.

Yang, Y., Jiang, J., Lu, X., Ma, J. and Liu, Y. (2015) Production of Sulfate Radical and Hydroxyl Radical by Reaction of Ozone with Peroxymonosulfate: A Novel Advanced Oxidation Process. Environmental Science & Technology 49(12), 7330-7339.

Yang, Y., Lu, X., Jiang, J., Ma, J., Liu, G., Cao, Y., Liu, W., Li, J., Pang, S., Kong, X. and Luo, C. (2017) Degradation of sulfamethoxazole by UV, UV/H2O2 and UV/persulfate (PDS): Formation of oxidation products and effect of bicarbonate. Water Research 118, 196-207.

Yang, Y., Pignatello, J.J., Ma, J. and Mitch, W.A. (2014) Comparison of halide impacts on the efficiency of contaminant degradation by sulfate and hydroxyl radical-based advanced oxidation processes (AOPs). Environmental Science & Technology 48(4), 2344-2351.

Yang, Y., Pignatello, J.J., Ma, J. and Mitch, W.A. (2016) Effect of matrix components on UV/H2O2 and UV/S2O82− advanced oxidation processes for trace organic degradation in reverse osmosis brines from municipal wastewater reuse facilities. Water Research 89, 192-200.

Yu, H., Nie, E., Xu, J., Yan, S., Cooper, W.J. and Song, W. (2013) Degradation of Diclofenac by Advanced Oxidation and Reduction Processes: Kinetic Studies, Degradation Pathways and Toxicity Assessments. Water Research 47(5), 1909-1918.

Zhang, R., Sun, P., Boyer, T.H., Zhao, L. and Huang, C.-H. (2015) Degradation of Pharmaceuticals and Metabolite in Synthetic Human Urine by UV, UV/H2O2, and UV/PDS. Environmental Science & Technology 49(5), 3056-3066.

Highlights:

- Propranolol degradation is comparatively studied in UV/H_2O_2 and UV/PDS
- $CO_3^{\bullet-}$ and Cl-containing radicals react with propranolol
- $^{\bullet}OH$ induces hydroxylation of propranolol at either amine or naphthalene group
- $SO_4^{\bullet-}$, $CO_3^{\bullet-}$ and Cl-containing radicals attack the naphthalene group
- $SO_4^{\bullet-}$, $CO_3^{\bullet-}$ and Cl-containing radicals generate more toxic products than $^{\bullet}OH$